

NOTE

Pointed Taylor Bubble Revisited

1. INTRODUCTION

The Taylor bubble problem consists of two fluids: a gas of negligible density in the interior of the bubble and an incompressible nonviscous fluid in the exterior of the bubble. The bubble is symmetric and infinitely long which rises under gravity at a speed U through a tube of width h . The dimensionless speed of the bubble is known as Froude number (F) and $F = U/\sqrt{gh}$. Here g is the gravitational acceleration. This bubble models the late stages of pure Rayleigh–Taylor instability.

The flow exterior of the bubble interface in the incompressible fluid is a potential flow which in theory would allow the free streamlines at the stagnation point (i.e., tip of the bubble) to separate at any arbitrary angle, θ_t . In the absence of surface tension, conservation of energy of fluid particles on the bubble interface (i.e., Bernoulli's equation) allows the bubbles, if they exist, to be either round, cusped, or pointed with $\theta_t = 120^\circ$ at the tip (see [4]). There is a general consensus that these bubbles exist as solutions of this problem.

The numerical solutions of Vanden-Broeck [9] show a pointed bubble rising at a speed $F = 0.3577$. This is consistent with a conjecture of Garabedian [5].

There are still some open questions about the pointed bubble. The equations of this problem contain F as a free parameter. Vanden-Broeck [9] uses a Fourier collocation method and determines F numerically by treating F as a free parameter. He finds $F = 0.3577$. He resolves this problem but with the value of F prescribed a priori. He attempts to find pointed bubbles for values of F other than 0.3577. The results lead him to suggest that there are no other pointed bubbles.

In Section 3 of the paper, we present a higher order constraint at the tip which contains the selection mechanism of the tip angle 120° of the pointed bubbles. This constraint is referred to as “tip selection criterion” or TSC in short. The TSC allows computation of tip angle from local higher order derivatives at the tip. The computed tip angle should be equal to 120° for the correct pointed bubble.

We use the tip angle or equivalently a local higher order derivative at the tip as a continuation parameter in our numerical procedure to provide numerical evidence of the

unique pointed bubble. Our convergence studies show that this unique pointed bubble rises at a speed $S \sim 0.35784$, accurate up to four decimal places. This is consistent with the result of Vanden-Broeck [9] except that our estimate of the speed differs from Vanden-Broeck's in the fourth decimal place. Using a desingularization method [2], we obtain the same estimate of speed. We also investigate the nature of singularity at the tip of the bubble by studying the asymptotic behavior of the Fourier spectrum of this bubble.

The rest of the paper is as laid out as follows. The Section 2 contains the basic formulation of the problem. In Section 3 we describe the higher order constraint at the tip and describe the determination of tip angle from local higher order derivatives at the tip. In Section 4 we describe the numerical method. The numerical results are presented in Section 5 and are discussed in Section 6. Finally we conclude in Section 7.

2. FORMULATION

The following formulation after Birkhoff and Carter [1] has been discussed in more detail in Daripa [4]. With respect to the reference frame attached to the bubble, fluid upstream in a tube of width h has a speed U downward. With appropriate normalization (speed by U and time by (h/U)), far upstream (i.e., $x \rightarrow -\infty$) $q = 1$, $\theta = 0$, where q is the speed, θ is the flow direction, and the stagnation point (i.e., the apex of the bubble) is located at $x = y = 0$. It is useful to deal with this problem in an auxiliary circle plane, $|\sigma| \leq 1$, which is obtained by a conformal mapping of the potential plane image of the flow in the physical plane. This mapping maps the bubble surface onto upper semi-circle $\sigma = e^{i\alpha}$; $\alpha \in [0, \pi]$, the walls on the real axis and the flow domain onto the interior of the domain bounded by the upper semi-circle and the real axis. The image of the apex of the bubble is $\sigma = i$ (i.e., $\alpha = \pi/2$ on $|\sigma| = 1$) and that of the tail of the bubble is $\sigma = \mp 1$.

The complex function $\tau = \nu - i\theta$, where $\nu = \ln q$, is an analytic function of σ within the semi-circle and is continuous and real on the real axis since $\theta = 0$ on the walls. An appropriate representation of $\tau(\sigma)$ in $|\sigma| \leq 1$ is then given by

$$e^{\tau(\sigma)} = (1 + \sigma^2)^\gamma [-\ln C(1 - \sigma^2)]^{1/3} \times [-\ln C]^{-1/3} \exp\left(\sum_{n=1}^{\infty} a_n \sigma^{2n}\right), \quad (1)$$

where $0 < C < 0.5$, $\gamma = \theta_i/\pi \geq 0$ and the Fourier coefficients, a_n , are real. A derivative form of the Bernoulli's equation on the bubble interface in this circle plane is given by

$$\pi \tan \alpha e^{2\nu} \frac{d\nu}{d\alpha} + \frac{e^{-\nu}}{F^2} \cos \theta = 0, \quad 0 \leq \alpha < \frac{\pi}{2}. \quad (2)$$

The values of ν and θ , obtained from solving (2) subject to the harmonic conjugacy of ν and θ according to (1), determine the shape of the bubble from integrating

$$z_\alpha = -\frac{\cot \alpha}{\pi q} e^{i\theta}, \quad 0 \leq \alpha \leq \pi, \quad (3)$$

where $z = x + iy$. For partial validation of numerical solutions it is useful to note that the exact asymptotic shape of the bubbles for large x downstream:

$$x = -\frac{F^2}{2} (1 - 2y)^{-2}. \quad (4)$$

This can be obtained from using the conservation of mass (i.e., $(1 - 2y)q = 1$ for x large with (x, y) on the interface) and the Bernoulli's equation on the interface.

A value of θ_i used in the construction of numerical solutions of Eqs. (1) and (2) need not be the tip angle of the computed bubble unless validated by some other criterion. This is discussed and exemplified in detail in Daripa [4]. Below we provide such a criterion which is then used to provide numerical evidence of the unique pointed bubble and an estimate of its speed.

3. TIP SELECTION CRITERION

It is convenient to reformulate the interface condition (2) as

$$\frac{d}{d\beta} (q^3) = \frac{3}{\pi F^2} \tan \beta \cos \theta, \quad 0 \leq \beta < \frac{\pi}{2}, \quad (5)$$

where we have used $\beta = \pi/2 - \alpha$. At the tip both, q and $(q^3)_\beta$, are therefore zero regardless of the nonzero value of θ_i . It has been shown in Daripa [4] that selection of the nonzero values of θ_i is hidden in the next order derivative of q^3 at the tip. It follows from (5) that

$$\cos\left(\frac{\theta_i}{2}\right) = \frac{\pi F^2}{3} (q^3)_{\beta\beta\beta=0}. \quad (6)$$

For the pointed bubble ($\theta_i = 120^\circ$) we have from (6)

$$\frac{\pi F^2}{3} (q^3)_{\beta\beta\beta=0} = \frac{1}{2}. \quad (7)$$

It is useful to notice from this relation that $q = O(\beta^{2/3})$ which is consistent with 120° angle at the separation point since $\ln q$ and θ are conjugate harmonic functions. Therefore Eq. (7) is referred to as ‘‘tip selection criterion’’ (or TSC in short) [4]. Below, we compute left-hand side of (7) as a function of F and correct values of F are obtained by requiring that the left-hand side of (7) be equal to $\frac{1}{2}$ according to (7). In view of relation (6), our procedure uses the tip angle as a continuation parameter to show the uniqueness of the pointed bubble. In the process, we also give an improved estimate of the speed of the pointed bubble and characterize the singularity at its tip.

4. NUMERICAL METHOD

Following Birkhoff and Carter [1] and Vanden-Broeck [9], we used the following Fourier collocation method. We substituted $\gamma = \frac{1}{3}$ for the pointed bubble in (1) and the expressions for ν , θ and their derivatives from (1) into (2). This gives an equation containing F and an infinite number of Fourier coefficients a_n . In order to solve it numerically, only a finite number of Fourier coefficients are retained and this equation is applied at N equi-spaced points: $\alpha_I = (\pi/2N)(I - 1/2)$, $I = 1, \dots, N$. This gives a system of N nonlinear equations which is solved by Newton's iterations for N unknowns. Numerical convergence for a choice of N is achieved if the values of the unknowns do not change more than 10^{-8} between two successive Newton iterations. Once this is solved, values of q and θ at the mesh points are obtained from (1) and the bubble is obtained by integrating (3). Numerical solutions are obtained in this fashion for a sequence of values of N to test for convergence. The values of N unknowns and shapes of the bubble profiles corresponding to various values of N are tested for convergence. Numerical results of the next section fall into two categories depending on the choices of N unknowns: (i) N Fourier coefficients with F prescribed; and (ii) $N - 1$ Fourier coefficients and F .

We also verified our calculations using a desingularization method [2]. In this method, the variable τ in (1) is desingularized by explicitly subtracting off the singularities. This allows the use of equi-spaced points: $\alpha_I = (\pi/2N)(I - 1)$, $I = 1, \dots, N$, which includes the end points as collocation points, unlike the previous method. This allows a better resolution of the regions near the apex of the

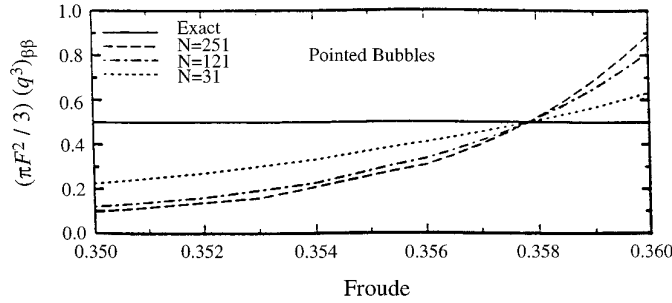


FIG. 1. Uniqueness of the pointed bubble: values of $(\pi F^2/3)(q^3)_{\beta\beta}$ at the apex of the numerically generated pointed bubbles vs the Froude number for various values of N . $(\pi F^2/3)(q^3)_{\beta\beta} = 0.5$ is the theoretical value at the apex of the pointed bubble.

bubble and is likely to generate more accurate solution. Results obtained with this method are also presented in the next section.

5. NUMERICAL RESULTS

5.1. Uniqueness

In Fig. 1 we plot numerical values of $(\pi F^2/3)(q^3)_{\beta\beta\beta=0}$ against F for various choices of N . Each of these curves intersects the line: $(\pi F^2/3)(q^3)_{\beta\beta\beta=0} = 0.5$ exactly at one value. As $N \rightarrow \infty$, the curve, F versus $(\pi F^2/3)(q^3)_{\beta\beta\beta=0}$, becomes steeper with increasing N crossing F axis at exactly one point. An extrapolation suggests that this point of intersection converges to a value $F \sim 0.35784$ as $N \rightarrow \infty$ which is correct up to at least four decimal places. This leads us to conclude that there is only one pointed bubble as solutions of the mathematical equations and that this bubble rises at a speed $F = 0.35784$ which seems to be accurate up to at least four places. In Fig. 2 we show the pointed bubble rising at speed $F = 0.357827$ when $N = 251$.

5.2. Speed

An accurate estimate of the speed, F_p , of the pointed bubble should be obtainable by cross-validating the results by different numerical methods. Therefore we computed the speed of this bubble in three different ways. We did not prescribe the value of F in the above numerical procedure. We treated this as a free parameter and computed its value by Newton's iteration. Our results suggest that estimate of the speed given above is correct. It should be pointed out that speed of the pointed bubble has been previously estimated to be 0.3577 using the same procedure [8]. The numbers in Table I in [8] are an increasing sequence of numbers and our improved estimate is consistent with the data in Table I of [8].

The value of speed computed by the desingularization method [2] is found to be insensitive up to four decimal

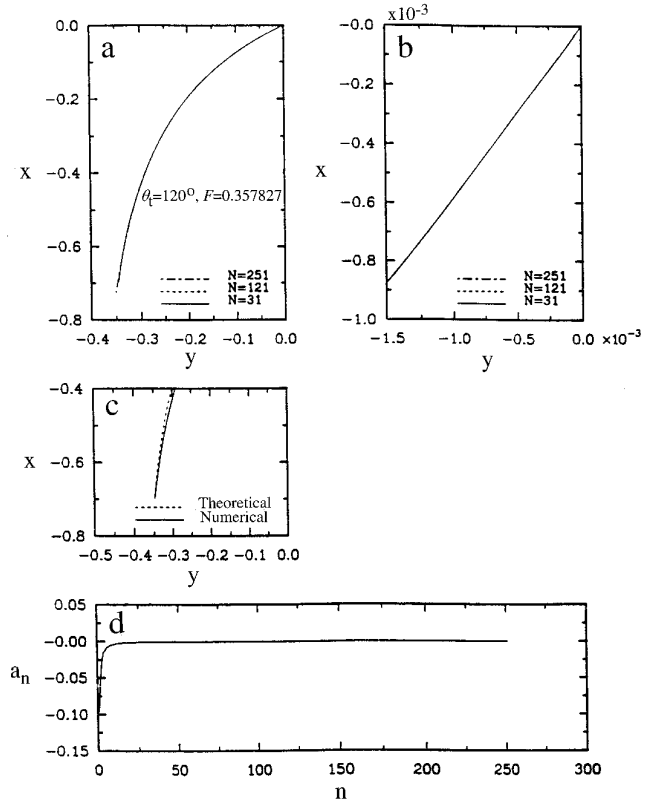


FIG. 2. The pointed bubble with $F = 0.357827$: (a) convergence of bubble profiles; (b) magnified view of (a) near the apex; (c) comparison of theoretical and numerical shapes of tails of the bubbles, $N = 251$; (d) behavior of Fourier coefficients, $N = 251$.

places. The following table shows the speed of the bubble computed by this desingularization method for various discretizations which further confirms our previous estimate of the speed.

5.3. Singularity

Characterization of the nature of the singularity at the tip of the pointed bubble is based on the asymptotic behav-

TABLE I
 F vs N in the
Desingularization Procedure

N	F
16	0.3584
32	0.3580
64	0.3578
128	0.3578
256	0.3578
512	0.3578
1024	0.3578

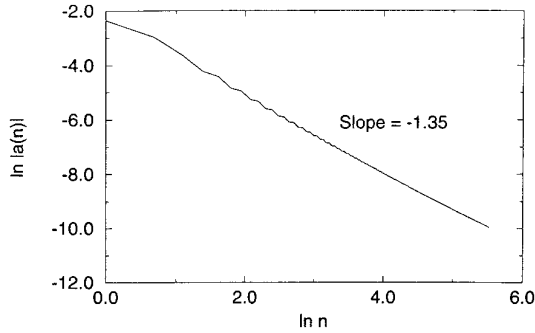


FIG. 3. Log-Log plot of the Fourier coefficients' amplitudes for the computed bubble in Fig. 2a. The straight line fit for high wave number modes has slope -1.35 .

ior of the Fourier coefficients a_n for this bubble. Plots of $\ln|a_n|$ versus $\ln n$ in Fig. 3 for the computed bubble in Fig. 2a suggests that $a_n \sim (n^{-1.35})$ as $n \rightarrow \infty$ for this pointed bubble. This estimate may be useful in the study of time dependent Rayleigh-Taylor instability.

6. DISCUSSION

The Fig. 1 clearly suggests that numerically generated bubbles for values of $F \neq F_p$ are not admissible pointed bubble solutions of Eqs. (1) and (2). These pointed bubbles for values of $F \neq F_p$ are artifacts of finite resolution calculations. However, it would seem from Fig. 1 that the plots for various N in this figure may approach the line $(\pi F^2/3)(q^3)_{\beta\beta=0} = 0$ for $F < F_p$ and $(\pi F^2/3)(q^3)_{\beta\beta=0} = 1$ for $F > F_p$. If this is the case, then TSC implies that these bubbles correspond to round bubbles for $F < F_p$ and cusped bubbles for $F > F_p$. This is consistent with the finding of Vanden-Broeck [9]. However, it is worth pointing out that our inferences here about the round and cusped bubbles from Fig. 1 is too far fetched and need further careful study. We do not pursue these studies here any further.

The fact that there are only round and cusped bubbles as solutions of Eqs. (1) and (2) for values of $F \neq F_p$ implies that solutions in Fig. 1 for these values of F have been generated with $\theta_t \neq \theta_a$, where θ_a is the correct tip angle. Fourier coefficients of such bubbles with correct F and incorrect values for θ_t in [4] were found to alternate in sign for high wave number modes and the origin of this generic behavior was traced in the logarithmic singularity at the tip of the bubbles. It seems logical that Fourier coefficients for these bubbles will also show similar behavior. Figure 4(a) shows this behavior.

In Fig. 4a, we plot the frequency, ν , of oscillations in the Fourier spectrum, against F over an interval including F_p for $N = 31, 121$, and 151 . A careful study of the magnified view of Fig. 4a near the region of sharp transition shows

that for each choice of N , there is only one window in F with no oscillations in the spectrum. This is shown in Fig. 4b. Figure 4b shows that this window size shrinks to zero with increasing N . We find that minimum and maximum values of F of this window, denoted respectively by F_{\min} and F_{\max} , become equal up to five decimal places for values of $N > 121$. Therefore we show the plot of F_{\min} versus $1/N$ in Fig. 4c. (Plot of F_{\max} versus $1/N$ collapses onto the same curve within the resolution of the plots for $N > 121$.) It makes sense to estimate the speed of this unique pointed bubble with monotonic decay rate of its Fourier coefficients by extrapolating the plot in Fig. 4c for $N \rightarrow \infty$. This bubble has a speed $F = 0.5784$ which is correct up to four decimal places as seen in this figure. Since this estimate is the same as our previous estimates of the correct solution, we conjecture that Fourier coefficients of the unique pointed bubble decays monotonically. The Fourier coefficients for the bubble shown in Fig. 2 decays monotonically.

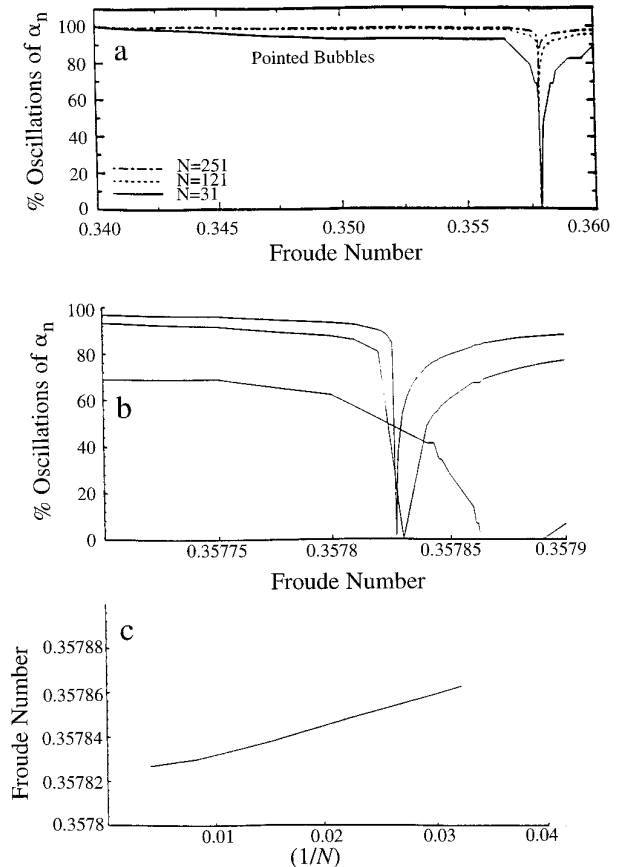


FIG. 4. Behavior of the Fourier spectrum of the pointed bubbles: (a) percentage of oscillations of Fourier coefficients as a function of the Froude number for various values of N ; (b) magnified view of (a) in the sharp transition region; (c) minimum value of the Froude number of pointed bubbles with 100% oscillations of Fourier coefficients vs $(1/N)$.

7. CONCLUSION

We have shown an application of the higher order constraint on the solution at the tip in establishing the uniqueness of the pointed bubble numerically. We have given an improved estimate of the speed of this pointed bubble. The best estimate of this speed is $F = 0.35784$ which is at least accurate up to four decimal places. The asymptotic behavior of the Fourier coefficients for this bubble is given by $a_n \sim n^{-1.35}$, accurate up to two decimal places.

ACKNOWLEDGMENTS

This research has been supported by NSF Grants DMS-8803669, DMS-9208061 and NASA under Contract NAS1-19480. The allocation of computer resources by the Texas A&M Supercomputer Center and NASA Langley Research Center is gratefully acknowledged.

REFERENCES

1. G. Birkhoff and D. Carter, *J. Math. Phys.* **6**, 769 (1957).
2. P. Daripa and L. Sirovich, *J. Comput. Phys.* **63**, 311 (1986).
3. P. Daripa, *Phys. Fluids* **6**, 1615 (1994).
4. P. Daripa, in *J. Comput. Phys.*, to appear.
5. P. R. Garabedian, *Proc. R. Soc. London Ser. A* **241**, 423 (1957).
6. P. R. Garabedian, *Commun. Pure Appl. Math.* **38**, 609 (1985).
7. M. A. Grant, *J. Fluid. Mech.* **59**, 257 (1973).
8. V. Modi, *Phys. Fluids* **28**, 3432 (1985).
9. J.-M. Vanden-Boreck, *Phys. Fluids* **29**, 1343 (1986).

Received April 26, 1995

PRABIR DARIPA

*Department of Mathematics
Texas A&M University
College Station, Texas 77843*